Al hematites prepared by homogeneous precipitation of oxinates: Material characterization and determination of the Morin transition

Article *in* Physics and Chemistry of Minerals · January 2002

DOI: 10.1007/s002690100201

CITATIONS
33

READS
70

6 authors, including:

Robert E. Vandenberghe
Ghent University
175 PUBLICATIONS **3,853** CITATIONS

SEE PROFILE

Vidal Barrón
University of Cordoba (Spain)
198 PUBLICATIONS **6,384** CITATIONS

SEE PROFILE

Phys Chem Minerals (2002) 29: 122–131
DOI 10.1007/s002690100201

ORIGINAL PAPER

G. M. da Costa · E. Van San · E. De Grave
R. E. Vandenberghe · V. Barrón · L. Datas

Al hematites prepared by homogeneous precipitation of oxinates: material characterization and determination of the Morin transition

Received: 19 April 2001 / Accepted: 25 June 2001

Abstract A novel method for synthesis of aluminium hematites, based upon the homogeneous precipitation of Fe and Al oxinates in various proportions, is presented. The precursor precipitates are heated in air at 700 °C. X-ray diffraction, thermal analyses, BET, FTIR, optical reflection analysis, TEM and Mössbauer spectroscopy at room temperature and 80 K of the resulting products indicate that single-phase hematites are formed with structural Al substitution of up to 10 at%. Interestingly, the particle size (> 100 nm) is not substantially reduced by the Al content. Although it remains difficult to obtain a homogeneously distributed Al substitution in the final hematite, this processing line offers a unique opportunity to separate the effects of grain size and Al substitution on the Morin transition temperature (T_M) of Al hematite. From the comparison between the present hematites and a series of Al-substituted hematites with lepidocrocite as precursor, it could be shown that the effect on T_M, associated with a change of a factor 10 in grain size, is about 1/3 of the effect caused by a change of 10 in the degree of substitution. Finally, it is suggested that proper thermal treatments under different conditions of the same precursors are likely to produce spinel phases.

Keywords Mössbauer spectroscopy · Al · Morin transition · Magnetic properties · Hematite

G. M. da Costa
Department of Chemistry,
Universidade Federal de Ouro Preto,
35400, Ouro Preto, Brazil

E. Van San (✉) · E. De Grave · R. E. Vandenberghe
Department of Subatomic and Radiation Physics,
NUMAT Division, Ghent University, 9000 Gent, Belgium
e-mail: erwin.vasan@rug.ac.be
Tel.: +32-9-264-65 70; Fax: +32-9-264-66 97

V. Barrón
Department of Agricultural Sciences and Resources,
University of Córdoba, 14080, Córdoba, Spain

L. Datas
CIRIMAT (LCMIE), Université Paul Sabatier,
F-31062 Toulouse, France

Introduction

Iron oxides and oxyhydroxides are widely spread in nature, occurring in soils, ores and rocks. Both synthetic and natural Fe oxides are being intensively used in industry as catalysts, pigments, magnetic recording devices etc. The most common compounds in these respects are hematite (α-Fe_2O_3), maghemite (γ-Fe_2O_3), magnetite (Fe_3O_4) and goethite (α-FeOOH). All of these occur abundantly in nature, and, as such, commonly contain foreign cations (e.g. Al) replacing iron in the structure. One can notice that increasing efforts have been devoted in recent years towards the search for new methods of synthesising these compounds, with particular emphasis on the incorporation of substituents. It is well documented that the crystal morphology, degree of crystallinity, surface area and many other properties are all strongly influenced by the synthesis route: The majority of these methods are based on the coprecipitation of the metal and iron, using a hydroxide (usually NaOH or NH_4OH) to adjust the appropriate pH (Schwertmann and Cornell 1991). However, this coprecipitation procedure has the inconvenience that inevitably the hydroxide is added in such a way that the OH^- concentration is momentarily not homogeneous throughout the reaction vessel, thus resulting in products which commonly consist of particles with a broad size distribution. An additional problem is that the incorporation of foreign cations tends to cause a significant lowering of the mean particle size, as is well documented to be the case for aluminous hematites and goethites (De Grave et al. 1982). Moreover, the effects of increasing Fe substitution on the one hand and of decreased crystal size on the other, upon the various magnetic properties of the oxides, are concomitant. Hence, it is extremely difficult to determine exactly what the intrinsic influence of each of these variables is.

(Vogel 1961)

Metal	Initial precipitation	Complete precipitation
Fe	2.5	4.1–11.2
Al	2.9	4.7–9.8
Ni	3.5	4.6–10.0
Ti	3.6	4.8–8.6
Co	3.6	4.9–11.6

Oxin (8-hydroxyquinoline) is a powerful complexing agent that can react with an enormous variety of cations, forming compounds of the type $M(C_9H_6ON)_n$, where n can be equal to 2, 3 or 4 (Vogel 1961). The precipitation is governed by the pH of the solution, as indicated in Table 1. From this table it can be seen that some cations, which are likely to replace iron in the structure of the oxides, can be precipitated in the same pH range as iron. This feature, and being aware of the possibility of generating OH^- groups in situ by the decomposition of urea, prompted the authors to examine this method for the synthesis of various metal-substituted Fe oxides. This contribution specifically concerns the results for Al substitution in hematite, α-Fe_2O_3. It is very likely, though, that the oxinates can also be used to prepare substituted magnetite and maghemite.

In the second part of this paper, attention will be focused upon the way in which the magnetic properties and especially the Morin transition (MT) of these oxinate-based hematites are influenced by this organic preparation method. A short overview of the theories related to MT can be found in Van San et al. (2001). The present oxinate-based oxides are compared to a previous series of HLEX Al-substituted hematites of the latter authors. The HLEX were prepared by heat treatment of Al-substituted lepidocrocite. Although obtained in a way that they contain only a low amount of hydroxyl groups, the other structural properties of HLEX are closely related to most of the high-temperature Al hematites described in literature. As grain size and substitution are linked, their intrinsic impact on the MT cannot be distinguished.

Materials and methods

Since oxin is almost completely insoluble in water, a solution was prepared by dissolving 100 g of the reactant in 1.0-l of acetic acid 2 M. Subsequently, ammonium hydroxide was added drop-wise until turbidity appeared. Next, a minimum amount of acetic acid was added to make the solution clear. This solution was then kept in a dark bottle that ensures stability over a long period of time.

Appropriate amounts of $FeNH_4(SO_4)_2 \cdot 12H_2O$ and $AlNH_4(SO_4)_2 \cdot 12H_2O$ were dissolved in a mixture of 10 ml HCl and 500 ml of distilled water, and the whole is poured into a 2-l round bottomed flask. About 130 ml of the oxin mixture and 35 g of urea are added to the flask, which is connected to a Liebig condenser. This solution is boiled for 2 h, after which the pH rises from 2 to 4. The products are filtrated, washed several times with water and finally dried at 100 °C for 24 h. All iron-containing oxinates are black, whereas the pure aluminium oxinate is light green. Subsequent combustion of these products to obtain the hematite was performed at 700 °C in a tubular furnace under constant air flow. The precursors are henceforward named RDX, and the fired samples RDXC, where X is the atomic % (at%) of Al-for-Fe substitution. When appropriate to express the Al concentration on a scale between 0 and 1, the symbol x will be used.

Simultaneous thermogravimetric analysis (TGA) and differential thermal analysis (DTA) of the combustion processes were performed in a Du Pont SDT2960 module. The temperature ranged from 25 to 800 °C, using a constant flow of synthetic air (100 ml min^{-1}) and a heating rate of 10 °C min^{-1}.

The specific surface areas of the resulting oxides were measured by the BET method using nitrogen adsorption in a Micrometrics Flowsorb 2300 apparatus. Transmission electron microscopy was performed in a Jeol 2010 TEM/scan apparatus equipped with an EDX detector. Since the particles are of the order of μm, EDX measurements in a TEM equipment are well suited to investigate the distribution and incorporation of Al in the oxide. Besides "overall" measurements on whole deposits, local EDX measurements (nm scale) inside selected oxide agglomerations were performed.

Powder X-ray diffraction patterns (XRD) were obtained with a Philips diffractometer with FeK_α radiation and a graphite monochromator. The samples were scanned in the range of 20–80° (2θ) with a step of 0.05° (2θ) and a counting time of 10 s^{-1} step. Silicon (ASTM no. 640) was used as an internal standard. The unit-cell parameters were calculated from the positions of the six principal peaks, which were computer-fitted with a standard minimisation routine.

The FTIR spectra in the range 400–600 cm^{-1} were measured on a MIDAC FTIR spectrometer. Samples for these studies were dispersed in (preheated) KBr pellets, about 1 mg in 300 mg KBr. The spectral manipulations of baseline adjustment, smoothing and normalisation were performed using the software package GRAMS (Galactic Industries Corporation, New Hampshire, USA). Band-component analyses were carried out with Gaussian line profiles.

Optical reflectance measurements were determined with a Varian Cary 1E spectrophotometer equipped with a diffuse reflectance attachment. To prevent orientation and saturation effects, the measurements were carried out on homogeneous mixtures of 3 wt% RDXC, 97 wt% $BaSO_4$. The reflectance (R) values were taken at intervals of 0.5 nm in the range 380–710 nm. The second-derivative curves of the Kubelka-Munk reemission function, $[(1 - R)^2/2R]$, were obtained according to a method described by Scheinost et al. 1999. Minima in these curves quantify the positions of the absorption bands due to Fe^{3+} ligand-field transitions and transitions due to magnetically coupled Fe^{3+} in adjacent sites (Sherman and Waite 1985) and hence reflect the presence of substituting cations.

Once the hematite characteristics were well established, the influence of their unusual properties upon the behaviour of T_M was investigated. Mössbauer spectra (MS) were collected between 80 K and RT with a time-mode spectrometer and constant-acceleration drive with triangular reference signal. Velocity calibration was achieved from the MS of a standard α-Fe_2O_3 absorber at RT. The velocity increment per channel was ~0.045 mm s^{-1}. Spectra were collected until an off-resonance count rate of $\sim 10^6$ was reached. They were analysed with Lorentzian-shaped symmetrical sextets for which the hyperfine field, H_{hf}, the centre shift, δ, and the quadrupole shift, $2\varepsilon_Q$, were adjustable parameters, as well as two width parameters, Γ and $\Delta\Gamma$ (De Grave and Vandenberghe 1990).

Results

The TGA curves are similar for all the precursor samples, and the plots for RD0, RD16 and RD100 are shown in Fig. 1. The evolution of the specific surface area of the hematite particles in function of the aluminium concentration can be described by Eq. (1)

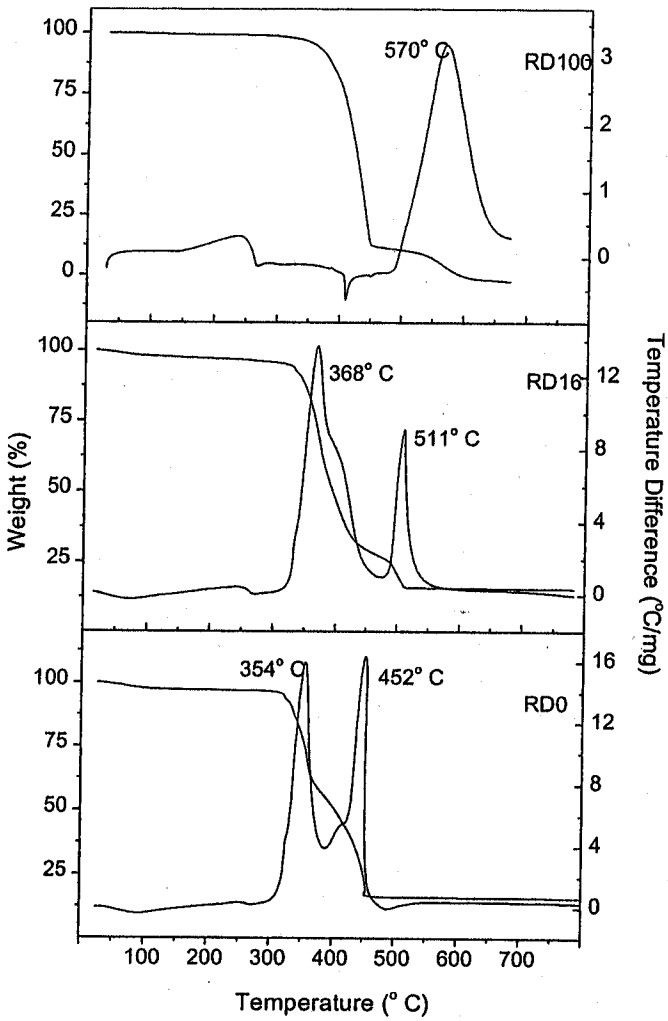

Fig. 1 TGA and DTA curves for iron oxinate (RD0), aluminium oxinate (RD100) and a co-precipitate RD16

$$S_{\mathrm{RDXC}}(\mathrm{m^2\ g^{-1}}) = 0.84 + 0.37 \times X \quad (r^2 = 0.96)\ , \qquad (1)$$

while the morphology of the RDXC series was visualised in Fig. 2. Table 2 and Fig. 3 give an overview of the corresponding statistical EDX study.

Numerical results on the (rhombohedral) crystallographic unit cells are collected in Table 3 while the FTIR spectra of RDXC in the region 400–600 $\mathrm{cm^{-1}}$ and the second derivatives of the optical reemission function $(1 - R^2)/2R$ in the visible range are collected in Figs. 4 and Fig. 5, respectively.

Figure 6 gives the evolution of the hyperfine fields in function of X. Two definitions, explained in the discussion section, were used to calculate the T_M temperatures (Fig. 7) from the fitted spectra. T_M(I) values are compared to the corresponding results of HLEX (Fig. 8) and to the data of the rhombohedral unit cell (Fig. 9). Finally, to examine the impact of surface effects, an integral low energy electron Mössbauer spectroscopy spectrum (ILEEMS, Belozerski 1993) was measured on RD0C (Fig. 10).

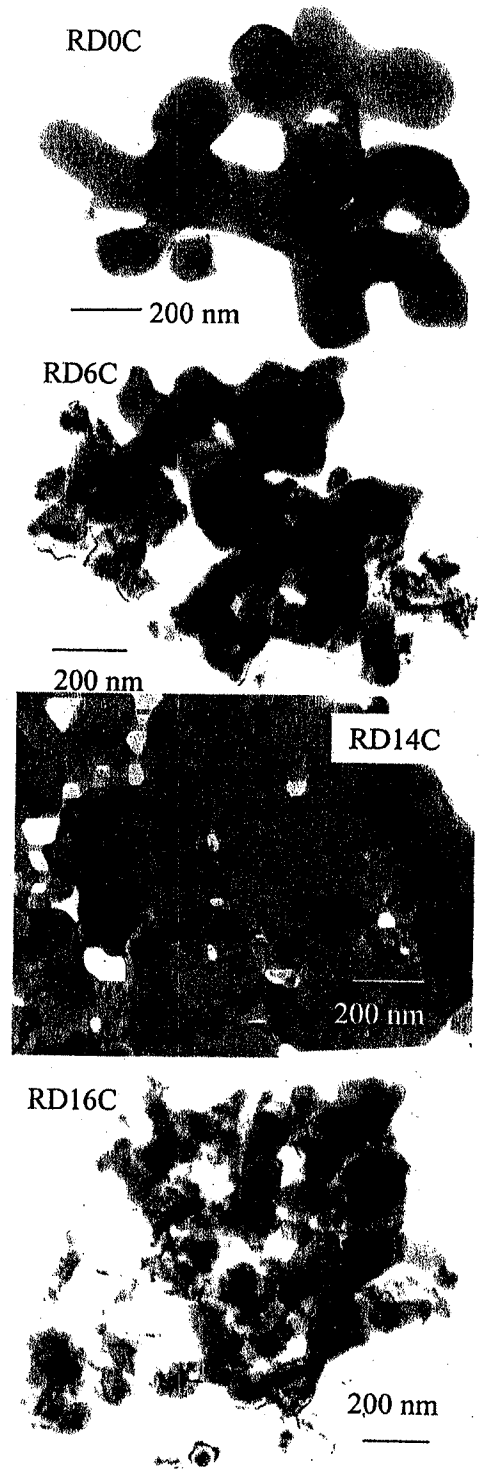

Fig. 2 TEM pictures of selected samples

Discussion

The total weight loss during the firing of the iron-containing complexes (Fig. 1) is about 81%, which is in good agreement with the theoretical value (83.6%) calculated according the reaction equation:

analyses performed on the Al concentration of RDXC

RDXC X	Mean of agglomerates (at% Al[a])	95% – interval of local probe analysis (at% Al[a])	Presence of corundum at the grain bounderies
0	–	–	–
2	1.9	0.93–2.35	No
4	3.5	2.80–5.28	No
6	6.3	2.15–10.5	Yes (area's with 60% Al)
8	5.8	4.81–7.03	Yes
10	6.8	4.8–14.4	Yes
12	12.9	7.6–14.0	Yes (limited)
14	14.5	10–17	No
16	14.0	9–9	No

[a] at% Fe + at% Al = 100%

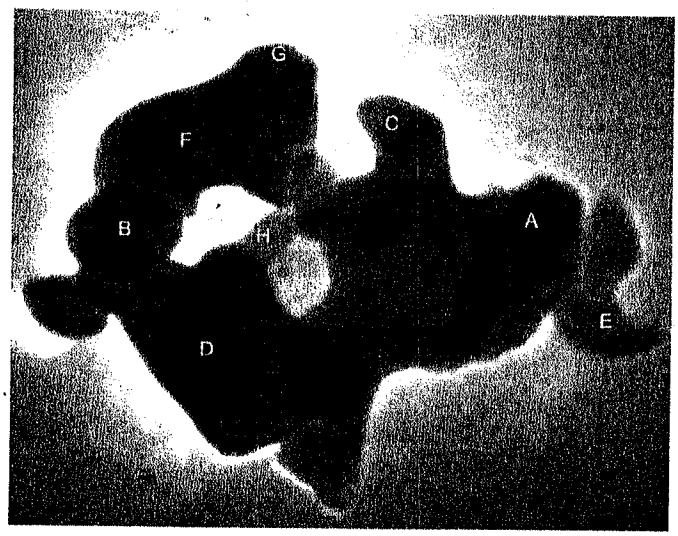

Fig. 3 Local EDX analysis on agglomerate of particles in RD4C (12000 x). Atomic percentage of Al (%Al + %Fe = 100%): *A* 3.96; *B* 3.09; *C* 6.27; *D* 2.48; *E* 6.45; *F* 2.83; *G* 7.08; *H* 6.79

$2(Fe_{1-x}Al_x)(C_9H_6ON)_3 \rightarrow \alpha\text{-}(Fe_{1-x}Al_x)_2O_3$. On the other hand, the Al-oxinate showed a loss of 100%, which can be explained by the fact that several oxinates, including the Al one, are volatile (Vogel 1961). With respect to RD0C, the decomposition peaks of RD16C are shifted to higher temperatures, a trend observed for all mixed oxinates, and suggesting that the aluminium ions were indeed coprecipitated with the iron and that they render the precursor's structure more stable.

Al also has a (minor) influence on the specific surface area of RDXC (Eq. 1). The order of magnitude of S_{RDXC} is an indication that the particles are quite large and free of pores. As a comparison, hematites prepared by dehydroxylation of oxyhydroxides at temperatures lower than 500 °C have surface areas up to 100 $m^2\ g^{-1}$ (Cornell and Schwertmann 1996). The morphology of the RD0C sample (Fig. 2) consists of ellipsoidal particles, sintered together to form a sort of sponge structure with typical dimensions around 1 to 2 μm. To about 10 at% Al substitution this structure remains, but the particles become more rounded off and disc-like, still with very large dimensions (at least 0.5 μm). From

Table 3 Lattice constants a and c, d_{104} and d_{110} interplanar spacings and line widths ($FWHM_{d104}$) of RDXC. All parameters in nm, except the line width, which is given in 2θ units. *Numbers between brackets* are the standard deviation for 95% of confidence

X (mol%)	a	c	d_{104}	d_{110}	FWHM
0	0.5038 (1)	1.3759 (5)	0.2701	0.2519	0.15
2	0.5033 (1)	1.3742 (3)	0.2699	0.2517	0.16
4	0.5029 (1)	1.3727 (3)	0.2696	0.2515	0.17
6	0.5027 (2)	1.3718 (7)	0.2695	0.2514	0.19
8	0.5023 (2)	1.3702 (7)	0.2692	0.2512	0.19
10	0.5021 (1)	1.3701 (6)	0.2691	0.2510	0.20
14	0.5016 (3)	1.3675 (6)	0.2688	0.2508	0.26
16	0.5013 (1)	1.3669 (7)	0.2686	0.2506	0.20

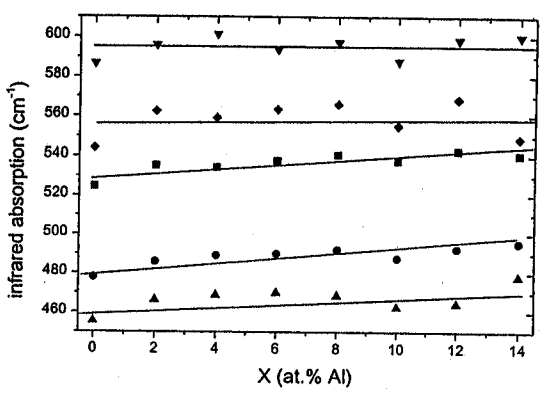

Fig. 4 Some fitted infrared absorptions of the RDXC hematite series in function of Al subtitutions

10 at% Al onwards, more compact "grid plates" of agglomerated round particles are formed with dimensions quickly reducing to a bottom value of 100 nm (RD14C), then remaining around that value for higher X (Fig. 2, RD16C).

Based on the EDX results (Table 2), the RDXC series can be divided into three regions: RD0C–RD6C, RD6C–RD10C and then from 10 at% Al onwards. In the region $X = 0$–4, the overall composition of the sample closely approximates the aimed composition, although inside the particles some large variations can occur from point to point. This was already mentioned

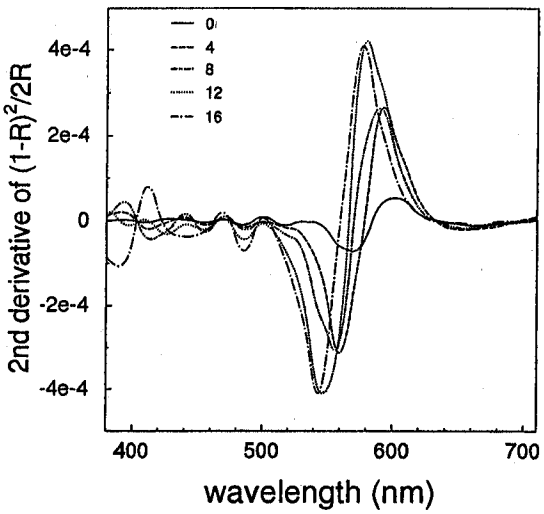

Fig. 5 RDXC series: second derivative of the diffuse reflectance in function of aluminium substitution

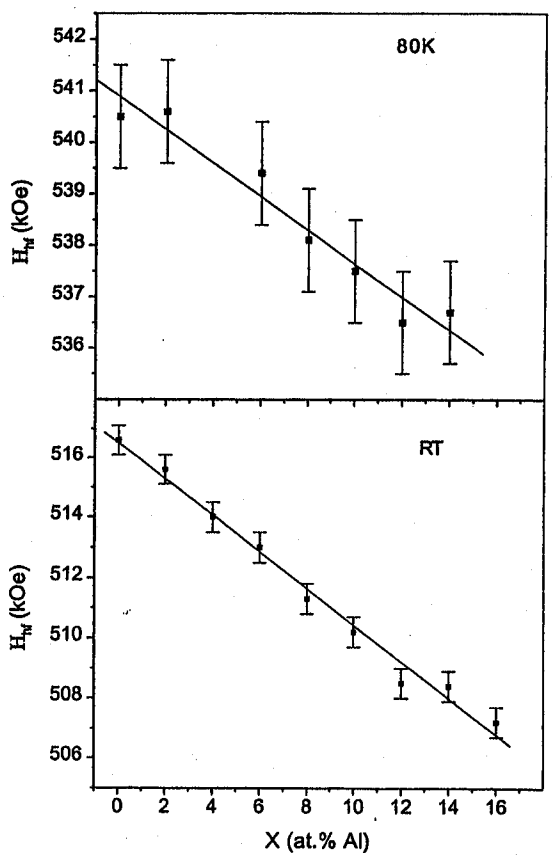

Fig. 6 Effect of the aluminium substitution on the room temperature (*bottom*) and 80 K (*top*) hyperfine fields of hematite. *Solid lines* are the best linear fits to the data

by De Grave et al. (1988) for hematite with goethite precursors. It can be further illustrated in Fig. 3, representing a particle of RD4C. The letters on the figure indicate where a local EDX analysis was performed. In the centre of the particles (A, B, D, F), the oxide is

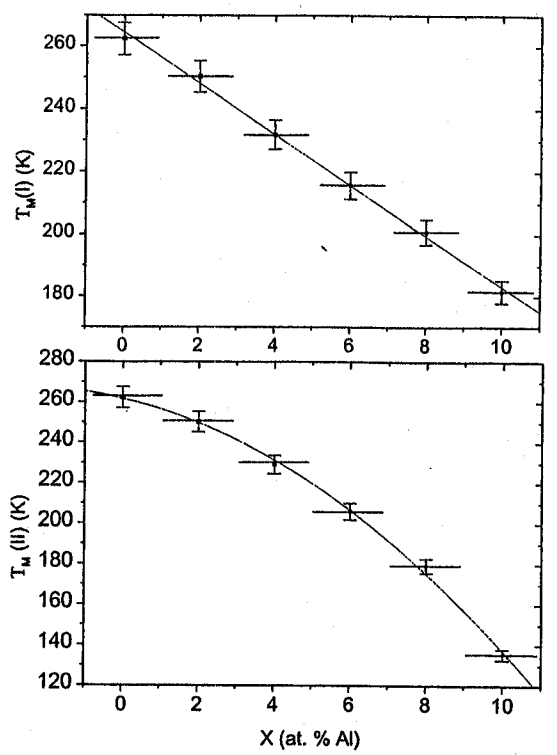

Fig. 7 T_M in function of Al substitution. *I* and *II* are explained in the text

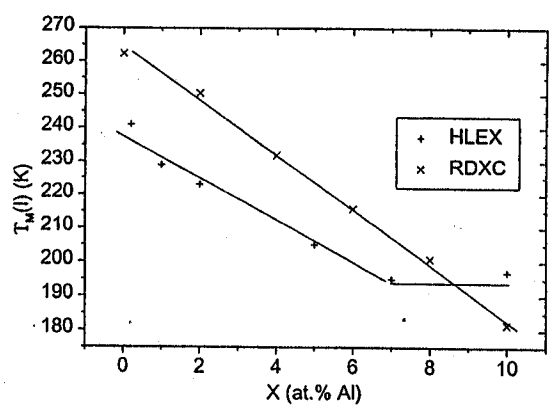

Fig. 8 Comparison between *X* (at% Al) and T_M(I) for HLEX and RDXC hematite

thicker and the beam will pass through a volume element with lower surface to bulk ratio compared to the outer parts of the particles (C, G, H and E), where the beam practically reaches only the outer layer of the sample. It can readily be observed that a significant gradient exists in the grains (from 2.5 at% Al in the core to 7.08 at% Al at the edges). In global EDX analysis, from 6 at% Al onwards, it can be observed that the Al concentration, which is integrated in the oxide, remains about 2% below the anticipated value as a consequence of the presence of corundum *outside* the oxide particles. Over 10 at% Al, where the morphology of the oxide changes

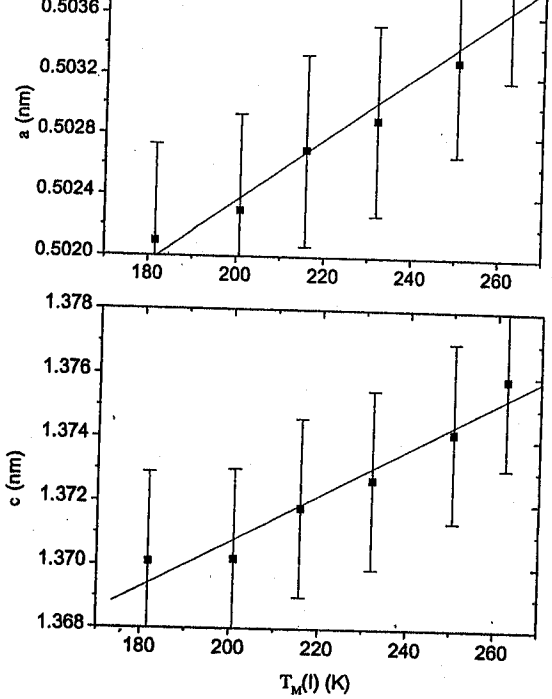

Fig. 9 Relation between $T_M(I)$ and the rhombohedral unit cell parameters a and c of the hematite

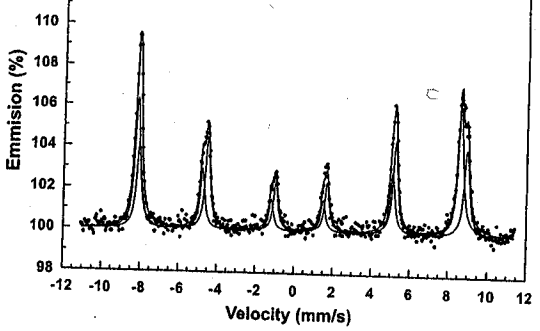

Fig. 10 ILEEMS spectrum of RD0C, 260 K

to smaller particles, the corundum phase, however, is no longer detected as a separate phase. In summary, the dimensions of the individual subgrains are linked to the distribution of Al. It further seems that the Al is preferentially present in the outer layers of the grains.

XRD spectra show only the peaks corresponding to hematite, except for the excluded sample RD20C, that exhibits some additional reflections that can be attributed to either magnetite or maghemite. A gradual shift towards higher diffraction angles with increasing Al of all hematite lines again suggests that the vast majority of Al is incorporated into the hematite structure. The XRD-line widths (Table 3) of the two most intense peaks (hkl = 104 and 110, rhombohedral unit cell) are equal and increase from 0.15° (2θ) for the non-substituted sample to 0.20° (2θ) for sample RD16C (the instrumental width is 0.12°). This confirms once again that the mean particle sizes are larger than 100 nm for all compositions. These figures can be compared with those for Al hematites obtained from goethites (De Grave et al. 1988), where the line widths were reported to be 0.39° (0 mol% Al) and 0.52° (13.8 mol%), implying a substantial decrease in crystal size with increasing Al. Another consideration is the influence of Al on the a and c directions of RDXC. Linear least-squares fits result in the following equations:

$$a = 0.5036 - 1.484 \cdot 10^{-4} \times X \quad (n = 8, r^2 = 0.99) \qquad (2)$$

$$c = 1.3750 - 5.368 \cdot 10^{-4} \times X \quad (n = 8, r^2 = 0.98)\ . \qquad (3)$$

The values for both slopes are in close agreement with those obtained for Al hematites prepared from Al ferrihydrite (Schwertmann et al. 1979), or from Al goethites (De Grave et al. 1982; Wells et al. 1989). This means that the influence of Al on the lattice parameters of Al-substituted hematite seems to be independent of the preparation route.

As a function of the Al content, the two RDXC IR bands around 460 cm^{-1}, (more pronounced) 480 and 530 cm^{-1} (Fig. 4) have a tendency to rise in frequency, which is comparable to the behaviour of the HLEX series (Van San et al. 2001) and logical since both bands correspond to Fe–O lattice vibrations (Wolska and Szajda 1988) that shift towards corundum values. Contradictorily to what is usually observed, the RDXC band around 600 cm^{-1}, attributed to –OH groups using the data of the same authors, does not undergo a variation with the Al concentration. This finding can be understood on the basis of the preparation method: RDXC is formed during a short and violent firing of a water-insoluble organic complex at 700 °C. Therefore, an important OH^- incorporation, enhanced by the presence of Al, is not an issue here.

The amplitudes of the second derivatives of the Kubelka-Munk curves (Fig. 5) increase with rising Al substitution, which is the behaviour opposite to that of the HLEX series. This could be an effect of crystal size and shape. While the crystal size of the HLEX is reduced for orders of magnitude and the shape changes from ellipsoidal to rounded disc-like particles, RDXC is characterised by µm-like irregular and agglomerated structures, becoming somewhat finer in their substructure, but their dimensions are surely not reduced to the same extent. In line for both series, however, are the shift of the minima of the second derivatives to lower frequencies (= influence of Al on the covalence of the Fe–O bonds) and the rise of the A485/A550 area ratio when exchanging iron. The latter area ratio is, in fact, the ratio between a signal (485 nm) of "goethite-like" behaviour, i.e. goethite-typical Fe^{3+} electronic transitions due to the presence of OH^- groups or occluded Al substitution atoms on the one hand and a corresponding "pure hematite" Fe^{3+}–Fe^{3+} pair excitation (550 nm) on the other (Galvéz et al. 1999). It should be stressed that

the first band is called a goethite-like behaviour, as no indication for the physical presence of this oxyhydroxide can be derived from any of the applied techniques. In our RDXC series this ratio mainly gives an idea about the rise in Al concentration in the more superficial layers of the oxides. Starting at a value of 0.019 ($X = 4$) the ratio rises to 0.044 ($X = 12$) and then saturates to 0.09 for $X = 14$ or higher, concurrently with the Al saturation of the outer oxide layers.

Additional conclusive evidence for the structural incorporation of Al into the RDXC hematite structure was found from the variation of the magnetic hyperfine field H_{hf} with Al content x, as obtained from MS (Fig. 6). The inclusion of a non-magnetic ion is expected to produce a decrease in H_{hf} because of the loss of some Fe–O–Fe exchange paths, causing a decrease in the average supertransferred hyperfine field. An excellent linear correlation is found between H_{hf} (in kOe) and x for x up to 0.16

$$H_{hf}(\mathrm{RT}) = 516.5 - 61x \quad (n = 9, r^2 = 0.99) \ , \tag{4}$$

$$H_{hf}(80\,\mathrm{K}) = 540.8 - 32x \quad (n = 9, r^2 = 0.98) \ . \tag{5}$$

As can be seen from Eq. (4), at RT the slope is −61 kOe, whereas for the Al hematites prepared from goethites this slope is −76 (Murad and Schwertmann 1986). This higher value might be due to the effects of Al substitution and smaller particle sizes for the latter sample series. Small particle size is indeed known to reduce the hyperfine field from the bulk value (Mørup 1984) and the combined effect of Al substitution and small crystal size was evaluated by Murad and Schwertmann (1986), who found that the hyperfine fields are better described by the multiple correlation (Eq. 6):

$$H_{hf}(\mathrm{RT}) = 517 - 76x - 330\mathrm{MCL}^{-1}\mathrm{c} \quad (n = 15, r^2 = 0.89) \ , \tag{6}$$

where MCLc is the mean coherence length in the c direction (nm). Equation (6) shows that for large particles (above 100 nm), which is the case for the present samples, the effect of crystal size on the hyperfine fields is much smaller than the effect of aluminium substitution. Caution, however, must be taken into consideration in comparing the absolute values of these equations, since the distribution of Al throughout a grain is likely to be inhomogeneous.

As a function of temperature (or external magnetic fields, not considered here), pure and well-crystallised hematite undergoes a magnetic spin-flip transition at $T_M \approx 265$ °C (Morrish 1994), well known as the Morin transition. Above the MT the spins, lying in adjacent basal (111) planes, are canted with respect to one another, giving rise to a weakly ferromagnetic (WF) state, whereas below T_M, the spins are aligned antiferromagnetically along the [111] axis. Structural defects, small particle sizes and cation substitutions all decrease the value of T_M, and eventually totally suppress MT (Fysh and Clark 1982).

It is very common that in substituted hematite powders the two spin states coexist over a wide temperature range (De Grave et al. 1983). This coexistence of two states at 80 K is clearly noticeable by the asymmetric peak depths of the outer lines. For sample RD4C, this asymmetry is only minor, and the AF and WF spectral components at 80 K cannot be resolved with reasonable reliability. Fitting parameters needed to be fixed. From $X = 6$ onwards, the AF fraction at 80 K is reduced in a practically linear way.

Up to now, it was considered that both small particle size and Al substitution affect the MT of hematite in a concomitant way. Since higher Al commonly implied smaller particles (Schwertmann and Cornell 1991, Cornell and Schwertmann, 1996), it has not been feasible so far to accurately quantify the effects of each of the parameters separately. The finding that the particle size of the sub-particles for the present sample series does not decrease substantially below 100 nm even at the highest values of Al substitution, provides a unique opportunity to examine the effect that Al exerts upon the magnetic properties of these hematites in function of temperature. First, we consider the definition of the Morin transition temperature T_M. One could define the latter in several ways. One view, called definition I, is to regard the point where the fraction of AF phase in the fitted MS is reduced to 50% of its original saturation value at low temperature. In practice, this corresponds to its value at 80 K. A second, alternative definition (II) of T_M is the temperature at which exactly 50% of the spectral area can be attributed to an AF phase. It can be noted (Fig. 7) that the first definition yields a perfectly linear behaviour of T_M as a function of the nominal substitution degree, while definition II produces a quadratic relationship with X.

There is no straightforward theoretical basis to assume whether a relationship between the presence of diamagnetic substituents and the corresponding change of T_M should be linear, quadratic or even of higher order. So which definition is the best cannot be determined a priori. Nevertheless, some indications can be retrieved. Literature data report most T_M either to be above 180 K or to be absent (see Vandenberghe et al. 2001, in press for unsubstituted hematites). Comparison of the RDXC data with the previously prepared HLEX series reveals the $T_{M,HLEX}$ to be systematically about 20 K lower than the corresponding $T_{M,RDXC}$ as long as the Al substitution is low enough to have a single AF phase at 80 K. Going from RD2C to RD4C or higher, the $T_{M,RDXC}$ data reported from definition I remain in line with these observations, while those from definition II fall rapidly below 180 K. Therefore, definition I can be taken as the most consistent one.

Another interesting parameter is the width of the transition region, i.e. the temperature interval ΔT_M, where the ratio between the relative spectral contributions of AF and WF gradually changes. Compared to pure, single-crystal hematite, where this transition region is limited to a narrow region of about 10 K, RDXC has

a ΔT_M going from 25 K (RD0C) to 150 K (RD10C). This behaviour can again be explained in view of the short reaction time to form the oxide and the resulting spongeous and irregular substructure of the material (TEM, Fig. 2). It is likely that the observed "transition width" is actually the accumulated result of the transitions of each of the particular subgrains of an agglomerate. One could therefore question whether the T_M, calculated from the MS spectra is still representative for a hematite sample with a certain aimed concentration of Al. The authors believe that it is, since the broadening of the transition region itself does not itself influence the obtained value of T_M. For example, the EDX Al analysis showed that the 95% concentration interval in which the local probe determinations within particles are situated is very broad, sometimes up to several atomic percentages; but a multitude of EDX measurements on each sample supports the idea that the same statistical number of areas with an Al concentration too low or too high with respect to the mean value can be found. Therefore, the calculated mean T_M remains unaffected. Local probe means here an order of magnitude of nm. In terms of MT, this means that for rising temperatures first the more Al-containing parts of the grains will go into transition, and at higher temperatures the less substituted parts. The idea of homogenization of the Al by an annealing treatment is probably not a solution for this problem, as one risks the expulsion of Al.

A next point of discussion is the comparison between RDXC and the more "traditional" lepidocrocite- and goethite-based α-$(Fe_{1-x}Al_x)_2O_3$. As already mentioned, it was observed that the values of T_M(I) are systematically up to 20 K higher than for the HLEX series (Fig. 8), an effect which is even more pronounced with respect to the goethite series (De Grave et al. 1988). The main macroscopical differences between these series are water content, grain size and morphology; but also the properties of the unit cell (dimensions, concentrations of defects, etc.) are to be considered, as Dang et al. (1998) suggest the latter to be the real parameters determining the presence of MT, rather than the grain size. The latter authors also focus attention on the importance of anisotropic changes in c and a. By annealing a hematite sample they differentiate between a first step where water loss causes isotropic changes of a and c and a second step where c decreases and a increases (loss of –OH and associated vacancies). An MT is occurring when a and c fall in a certain critical value region. To the extent of checking whether $T_{M,RDXC}$ is influenced by the unit-cell parameters a and c, Fig. 9 relates the latter with the T_M(I) values. From this figure, $T_{M,RDXC}$(I) is equally well linearly correlated to the unit cell parameters a ($r^2 = 0.97$) and c ($r^2 = 0.95$). Previously, Yamamoto (1968) found the correlation coefficient for a to be ten times stronger than that of c. It is believed that this finding is the result of OH^- incorporation. In further detail, the corresponding regression curves illustrate that a change in cell parameters has a stronger effect on T_M in the RDXC series than it had in the HLEX powders: the temperature change $\Delta T_{M,RDXC}$, resulting from an expansion of 1 nm in a, is 1.2 times higher than the corresponding effect for HLEX and for a unit change in the direction c, this effect being even more pronounced with a factor of 1.4. Thus, the different MT behaviour of both material series cannot be explained solely on the basis of a difference in the absolute values of a or c, to which anisotropy is very sensitive, because their respective unit cells are comparable. An alternative view would be to include the influence of structural incorporation of impurities. As all oxides were laboratory-prepared from analytical product mixtures, the only possible feasible inclusions are again protons, OH^- and H_2O. Obviously, the risk that hydroxyl is included in the structure is higher in HLEX, where the precursor material is precipitated from a wet solution, while oxinates are water-insoluble. Therefore, one would expect the MT to be more suppressed by hydroxyl in the HLEX line, especially at higher substitution degrees, where the possibility of water inclusion rises (Van San et al. 2001). On the contrary (see Fig. 13), the T_M(I) values of the RDXC tend to approach those of HLEX at higher Al amounts. Consequently, the presence of hydroxyl and its associated vacancies cannot explain the difference in transition behaviour.

One could also consider the possible effects of surface area, shape and surface anisotropy. For RD0C (Fig. 10), it was found that $T_{M,surface\ (ILEEMS)}$ is only 2 K below the "bulk" (transmission) value, proving that for RDXC, surface effects do not play an important role. Above 4% Al, no MT shows up in the RDXC-ILEEMS spectra, but the measurements do not allow conclusions on anything about the influence of surface anisotropy, since it was already illustrated that the Al concentration in the surface layers is much higher than in the bulk. One aspect remaining therefore is the interplay between shape and particle-size effect. As it was observed that the substructure of the RDXC grains becomes finer with higher Al for Fe replacement, and thus closer approaches the HLEX morphology, it is understandable that the respective transition temperatures come closer together. Because the MT is a macroscopically observed property, we believe it also to be more in line with expectations that not only unit-cell dimensions of the oxide but also "long-distance" characteristics play a role in the setting of its temperature.

For X above 10, one can observe (Table 4) that T_M(II) drops fast below 180 K, while T_M(I) surprisingly increases with X. As mentioned earlier, EDX measurements show that the more Al is added to the original oxinate-complex mixture, the more heterogeneously it is distributed throughout the oxide grains, with a significant enrichment towards the surface layers and even appearance of corundum. It is believed that the maximum Al concentration that can be incorporated in the oxide structure via the oxinate preparation method is of the order of 10%. Above this limit, the excess Al most probably agglomerates during the firing reaction in corundum dots that are intimately mixed with the iron

oxide in such a way that XRD and EDX cannot detect them as a separate phase. In this case, some Fe oxide around the corundum spots is likely to be depleted in Al, as the latter element prefers to diffuse out of the hematite structure to join the Al_2O_3 phase. These "low-Al" areas in turn lead to the existence of a remaining AF phase in the 80 K-MS, and hence to observable transition phenomena with changing temperature. The resulting "mean transition temperature value", however, will no longer correspond to the definition of the T_M temperature for Al hematite with that nominal Al concentration. This statement is supported by the fact that above $X = 10\%$, $T_M(I)$ increases with Al, as more corundum dots are formed and more Al from the oxide is given the occasion to diffuse to these dots. Below 10 at% Al, the corundum is well separated from the oxide in larger particles that have only limited interaction with the oxide structure, and the transition temperature remains representative for hematite with an Al concentration approaching the aimed value.

Additional comment

An interesting side effect of the oxin preparation method is the anticipation that the average particle size may be modified by changing the conditions of temperature and atmosphere under which the thermal treatment of the involved precursors is carried out. However, these changes may produce other phases as well, e.g. magnetite or maghemite (da Costa et al. 1994). Furthermore, if the oxinates cannot be transformed directly to a spinel phase, there is still an indirect way of producing these compounds: hematite can be mixed with sucrose and submitted to thermal treatments to produce maghemite (Bowen et al. 1994). Finally, it might also be possible that some other metals can be incorporated into the hematite structure, as suggested by the data of Table 1.

Conclusions

The proposed method, via oxinate precursors for the synthesis of hematites, produced samples that can incorporate up to 10 at% Al in their structure. An important result is that very large particles are produced, however at relatively high temperatures. The dimensions are on the average above 100 nm, an order of magnitude that is not substantially affected by the Al concentration. A disadvantage of the preparation method, however, is the heterogeneous distribution of aluminium in the large grains that are obtained, which is an inevitable consequence of the tendency Al shows to migrate outside the grain core at the applied temperature (De Grave et al. 1988). As a result, care should be taken concerning the exact stoichiometry of the Al-substituted hematite that can deviate by more than 1% from the initially aimed-at concentration. It is suggested that modifications in the thermal treatments can result in different average particle sizes or in the formation of other Fe phases such as magnetite or maghemite. This will be the subject of further research.

The obtained hematite has a structure not showing the disadvantage of incorporating additional water or hydroxyl groups, with associated vacancies, concurrently with the substitution of Al-for-Fe. Unit-cell parameters c and a of the rhombohedral unit cell of the hematite both correlate rather linearly with T_M, as determined with Mössbauer spectroscopy. This correlation is equally strong for a and c, contrary to the literature statement that a change in a would have a ten times stronger influence on T_M than c. It is suggested that this observation can be explained as resulting from the preparation-specific absence of hydroxyl. The changes in c and a over the whole of the substitution range remain nevertheless limited.

Since both the HLEX series, presented in an earlier paper (Van San et al. 2001), and the RDXC series have comparable unit-cell parameters, one can now distinguish the influence of shape/grain size and aluminium. By changing the Al concentration by 1 order of magnitude (from 1 to 10 at% Al substitution), $T_{M,RDXC}(I)$ changes about 73 K, while the "mean temperature difference"

$$T_{M,RDXC}(I) - T_{M,HLEX}(I) \ ,$$

between materials that differ about 1 order of magnitude in grain size is situated around 20 K for corresponding compositions. As a rule of thumb one can say that substituting Al for Fe in the oxinate-based hematites has a three to four times stronger influence on T_M than changing the grain size, structure or shape. The effect of surface anisotropy remains limited, as can be observed by comparison of ILEEMS and transmission Mössbauer spectra of unsubstituted material. Although it can be assessed beyond doubt that substitution is the most important parameter in setting the MT for the RDXC hematite series, shape, grain size and morphology do have an influence that cannot be neglected.

The oxinate preparation method is only suited for preparation of large grain hematites containing up to 10 at% Al that have representative magnetic properties; above this limit the Al tends to separate itself from the oxide, probably in the form of small dots, intimately mixed with the grain structure.

Acknowledgements This work was partially supported by CNPq and Fapemig (Brazil) and by the Fund for Joint Basic Research (Belgium). The authors wish to thank N.D. de Souza and R.H. Bahia (university of Ouro Preto, Brasil) for their assistance to the chemical preparation and Prof. Dr. A. Rousset, from the Université Paul Sabatier of Toulouse (France) for granting permission to use the BET facility of the CIRIMAT (LCMIE) Department. We also thank the FWO-Flanders (Belgium) (project G007.97) and the Belgian PAI/IUAP on small dimensions (P4/10) for their financial grants. V. Barrón is gratefully indebted to the Spanish Ministerio de Educación, Cultura y Deporte for a grant, allowing a 3-month study period at the NUMAT department, Ghent, Belgium.

References

Belozerski GN (1993) Mössbauer studies of surface layers, studies in physical and theoretical chemistry 81. Elsevier, Amsterdam

Bowen LH, De Grave E, Bryan AM (1994). Mössbauer studies in an external field of well-crystallized Al-maghemites made from hematite. Hyperfine Interact 94: 1977–1982

Cornell RM, Schwertmann U (1996) The iron oxides. VCH, Weinheim, p 101

da Costa GM, De Grave E, de Bakker PMA, Vandenberghe RE (1994) Synthesis and characterization of some iron oxides by sol-gel method. J Sol State Chem 113: 405–412

Dang MZ, Rancourt DG, Dutrizac JE, Lamarche G, Provencher R (1998) Interplay of surface conditions, particle size, stoichiometry, cell parameters and magnetism in synthetic hematite-like materials. Hyperfine Interact 117: 271–319

De Grave E, Vandenberghe RE (1990) Mössbauer effect study of the spin structure in natural hematites. Phys Chem Miner 17: 344–352

De Grave E, Bowen LH, Weed SB (1982) Mössbauer study of aluminium substituted hematites. J Mag Magn Mater 27: 98–108

De Grave E, Chambaere D, Bowen LH (1983) Nature of the Morin transition in Al-substituted hematite. J Mag Magn Mater 30: 349–354

De Grave E, Bowen LH, Vochten R, Vandenberghe RE (1988) The effect of crystallinity and Al substitution on the magnetic structure and Morin transition in hematite. J Mag Magn Mater 72: 141–151

Fysh SA, Clark PE (1982) Aluminous hematite: a Mössbauer study. Phys Chem Miner 8: 257–267

Galvéz N, Barrón V, Torrent J (1999) Preparation and properties of hematites with structural phosphorous. Clays Clay Miner 47: 375–385

Morrish AH (1994) Canted antiferromagnetism: hematite. World Scientific Publishing Company, Singapore

Mørup S (1984) Mössbauer spectroscopy applied to inorganic chemistry. In: Long GJ (ed) Plenum Press, New York 2: 89–123

Murad E, Schwertmann U (1986) Influence of Al substitution and crystal size on the room-temperature Mössbauer spectrum of hematite. Clays Clay Miner 34: 1–6

Scheinost AC, Schulze DG, Schwertmann U (1999) Diffuse reflectance spectra of Al-substituted goethite: a ligand field approach. Clays Clay Miner 47: 156–164

Schwertmann U, Cornell RM (1991) Iron oxides in the laboratory. VCH, Weinheim

Schwertmann U, Fitzpatrick RW, Taylor RM, Lewis DG (1979) The influence of aluminium on iron oxides. Part II. Preparation and properties of Al-substituted hematites. Clays Clay Miner 27: 105–112

Sherman DM, Waite TD (1985) electronic spectra of Fe^{3+} oxides and oxide hydroxide in the near IR to near UV. Am Mineral 70: 1262–1269

Vandenberghe RE, Van San E, Da Costa GM, De Grave E (2001) About the Morin transition in hematite in relation with particle size and aluminium substitution. Czech J Phys, in press (Vol 51)

Van San E, De Grave E, Vandenberghe RE, Desseyn HO, Datas L, Barron V, Rousset A (2001) Study of Al-substituted hematites, prepared from thermal treatment of lepidocrocite. Phys Chem Miner 28: 488–497

Vogel AI (1961) A textbook of quantitative inorganic analysis. Longman, London, p 128

Wells MA, Gilkes RJ, Anand RR (1989) The formation of corundum and aluminous hematite by the thermal dehydroxylation of aluminous goethite. Clays Clay Miner 24: 513–530

Wolska E, Szajda W (1988) The effect of cationic and anionic substitution on the α-$(Fe, Al)_2O_3$ lattice parameters. Solid State Ion 28–30: 1320–1323

Yamamoto N (1968) The shift of the spin flip temperature of α-Fe_2O_3 fine particles. J Phys Soc Jpn 24: 23–28